An Overview of Possibilities of Increasing the Permissible Speed of Underground Suspended Monorails for Transporting People in the Conditions of Polish Underground Mining

Jerzy Świder [1,*], Kamil Szewerda [1,*] , Jarosław Tokarczyk [1] , Franciszek Plewa [2], Aneta Grodzicka [2] and Krzysztof Kędzia [3]

1 KOMAG Institute of Mining Technology, ul. Pszczyńska 37, 44-101 Gliwice, Poland
2 Faculty of Mining, Safety Engineering and Industrial Automation, Silesian University of Technology, ul. Akademicka 2, 44-100 Gliwice, Poland
3 Faculty of Mechanical Engineering, Wrocław University of Science and Technology, ul. Wybrzeże St. Wyspiańskiego 27, 50-370 Wrocław, Poland
* Correspondence: jswider@komag.eu (J.Ś.); kszewerda@komag.eu (K.S.)

Abstract: The permissible speed of suspended monorails in underground mines is determined by the internal regulations of each country and depends on the type of transportation. In the case of passenger transportation, the maximal driving speed in Polish underground mining regulations is 2 ms^{-1}. Regarding the higher permitted driving speed in other countries, it is reasonable to consider changes to these regulations that would raise the permitted speed limit. Increasing the permissible travel speed would improve the efficiency of mining operations because of the significant reduction in the inefficient working time of miners traveling on the monorail from the shaft to their place of work. However, at the same time, an increase in the permissible speed of travel results in higher values of forces and accelerations affecting both the crew riding the train and the underground working infrastructure (the suspended route, slings, and arches yielding support). The results of the series of works carried out at the KOMAG Institute of Mining Technology to assess the impact of increasing the speed on the safety of both the crew and the mine infrastructure are presented in this article. For this purpose, several numerical simulations were conducted, considering the emergency braking of the suspended monorail during which the overloads are the greatest. The result of the simulations was the analysis of the effects of driving and emergency braking of the suspended monorail with increased travel speed on the following: the overloads acting on the crew being transported and the forces acting on the suspended monorail route, including the forces in each sling. Next, a potential solution for improving safety was developed. The development of the algorithm for an innovative method of sequential emergency braking of the monorail in the case of passenger transportation was one of the important solutions.

Keywords: underground mining; safety; mining monorails; transport; numerical simulations; travel speed; braking algorithm

1. Introduction

There are two types of transport in underground coal mines: the main one, related to the run-of-mine transport, and the auxiliary one, used for the transport of materials, machines, and people. The main transport machines used for run-of-mine transport are scraper conveyors and belt conveyors. With regard to auxiliary transport, currently, the most popular means of transport are underground railways and self-propelled suspended monorails. The main limitation of the underground railway is the ability to travel only with slight inclinations of the route (up to 4°). Suspended monorails have been used since the middle of the 20th century. Thanks to their advantages, such as no need to maintain the track on the floor (which can be difficult in situations of floor heave) or, in the case

of locomotives with their own drive, better mobility (possibility of reaching areas closer to the longwall panel), suspended monorails became popular [1]. Currently, both users and manufacturers of suspended monorails care about the continuous development of this means of transport. The development of suspended monorails requires interdisciplinary research work and is associated with the development of many industries. One of the directions of development results from the need to reduce the emission of exhaust gases in underground mines and is related to electromobility. In this regard, research work on introducing the electric drives to replace diesel drives [1,2] was started. The second aspect is the introduction of state-of-the-art and innovative control systems through the use of innovative mechatronic solutions [3–5]. Another area of development is focused on improving the current design so that suspended monorails can operate safely at higher speeds and the crew's driving comfort will increase [6,7]. In the light of changes resulting from the availability of coal deposits intended for mining and strategic changes consisting in the consolidation of mining plants, a significant extension of the distance that an employee has to cover from the shaft to the longwall face is observed. With the increase of this distance, the travel time of an employee in suspended monorails is significantly longer, which is an ineffective working time. This is unfavorable from the economic point of view. In order to increase the profitability of mines by extending the effective working time of miners, it is possible to increase the maximum permissible travel speed when moving personnel from the shaft to the workplace. Currently, Polish law allows people to travel at a speed of 2 ms^{-1}. However, according to the regulations, the emergency braking trolleys are automatically activated at the speed of 3 ms^{-1} [8]. Similar speed limits apply in mines in Slovenia. German mines use regulations according to which people can drive at a speed of 3 ms^{-1}. In Ukrainian mines, the driving speed is determined on the basis of manufacturer's specifications. In countries, such as Russia, China, Vietnam, or Mexico, the Polish railway manufacturers generally apply Polish regulations and limits.

Increasing the maximum speed of suspended transportation set is beneficial from the point of view of economy and work organization, due to the significant shortening of the personnel travel time to their place of work. On the other hand, one of the most important aspects of changing the regulations in this regard is the need to maintain the current level of safety, both for the suspended monorail operator and for the personnel travelling on this monorail. Due to legal and safety restrictions, it is not possible to test the suspended monorail at high speeds in in-situ conditions, in particular during emergency braking. The emergency braking was selected for the analysis, due to the greatest forces and overloads acting on the users and the mine infrastructure. As a part of the research work, pioneering in-situ tests were carried out, and then a numerical model of the selected suspended monorail was created for a several numerical simulations. The impact of the change in speed of the suspended monorail on acceleration acting on people in the monorail, the forces acting on suspensions of the monorail route, the vibrations in operator's cabin and the passenger cabin, and the amount of thermal energy generated in emergency braking were analyzed on the basis of the results. Then, concepts to minimize the risk of dangerous situations and improve the comfort of using suspended monorails were developed. It should be noted that the kinetic energy with which the suspended monorail moves is directly proportional to the square of the travel speed. Moreover, in the case of emergency braking, the higher energy loss is associated with occurrence of higher overloads affecting passengers in the monorail. According to the regulations, the deceleration acting on a person during emergency braking should not exceed 10 ms^{-2}. The deceleration acting on a person was calculated using numerical simulations with different variants of boundary conditions, in which the configuration of route suspension, the value and time process of braking force, braking starting speed were changed. Based on the results, it is possible to determine in which cases (configurations) the limit values are exceeded. One of the methods of analyzing the operator safety is using the calculated acceleration to numerical simulations with the virtual equivalent of the HYBRID III dummy (ATB—Articulated Total Body). Examples of research work using ATB models are presented in numerous

publications, e.g., [9–12]. This method has its origins in the automotive industry, where it is used to assess safety during crash tests. A study of the effect of collision speed on the probability of injury to a car's driver and passenger is provided in [13] as an illustration of how this method is used. Analysis of the effect of car seat vibrations on a child's comfort while riding in a car is another part of the employment of dummies in the automotive industry [14]. The issue of vibration is also very important in the context of a monorail operator workstation. The operator, for a significant part of working time, is exposed to vibrations resulting from the movement of suspended monorail along the rail. Because both the rollers and the rail are made of steel, every rail connection or unevenness on the monorail route is felt in the operator cabin. In order to protect against the effects of vibrations presented in [15–20], both stand tests and numerical simulations were carried out, which resulted in the suggestion of solutions to minimize the impact of vibrations on the monorail operator and passengers.

Another safety-related aspect concerning the mine infrastructure in terms of the increased energy to be dissipated during the braking process at higher speeds was the analysis of the forces in the route suspensions. The force is transferred to the steel arches of the roadway support through the route suspensions. The permissible load to a single arch in Polish mines is 40 kN. The literature contains descriptions of the behavior of roadway support arches under dynamic forces. These publications also cover aspects of transport with the use of suspended monorails [21–23]. In order to protect against the adverse effect of emergency braking on the roadway support at higher speeds, the impact of the way of suspending the monorail route, both on the braking deceleration and the forces transferred to the roadway support, was analyzed. The outcomes of the analysis provide the basis for the formulation of recommendations for the installation and stabilization of the monorail route designed for high-speed passenger transportation.

Another innovation in testing was the analysis of the temperature of brake shoes during emergency braking at increased speed. The results inspired the development of the concept of a new type of brake trolley.

Results of numerous studies conducted by the KOMAG Institute of Mining Technology about the potential of raising the permitted speed of suspended monorails are summarized in this paper (detailed results were published in earlier papers). This issue is particularly important in relation to the maximum travel speed when moving people.

2. Computational Model of Suspended Monorail

Specialists from KOMAG conducted pioneering tests, both on a test route built specially for this purpose (while driving at a speed of up to 5 ms^{-1}) and in-situ (up to the permissible speed, limited by law). The next step was the creation of a numerical model and its verification and validation using the results of in situ tests. Then, the computational model of the suspended monorail was extended, enabling the simulation of travel and emergency braking in the variants not possible on a real object.

2.1. Pioneering In-Situ Tests of Dynamic Quantities

A number of pioneering tests associated with dynamic phenomena during the operation of suspended monorails in underground mines were conducted by KOMAG specialists. The purpose of the tests was to collect data and analyses to gain knowledge in the following areas:

- real time processes for forces in the suspensions of the monorail route and the load to each roadway support arch under in-situ conditions,
- accelerations and vibrations affecting the monorail operator and the passengers,
- measurements of the brake shoes temperature during braking.

Dedicated force transducers were designed, manufactured, and installed in the suspensions of the monorail route for force measurement. Accelerations and vibrations of the transport unit travelling along the suspended route were recorded with the use of specialized measuring tools, provided by the KOMAG accredited Laboratory. The tests

were carried out in several locations, both on a test stand (a 90 m long test track, created as part of the INESI project) and under in-situ conditions (JSW Zofiówka and ZG Siltech mines). Dynamic quantities (forces, accelerations) were recorded both during the travel of the transport unit at different speeds through the test section and during emergency braking. The test sections were located in horizontal and inclined roadways. The model of the sensor and mounting method of the sensors in the suspension during in-situ tests is shown in the Figure 1 [11,24].
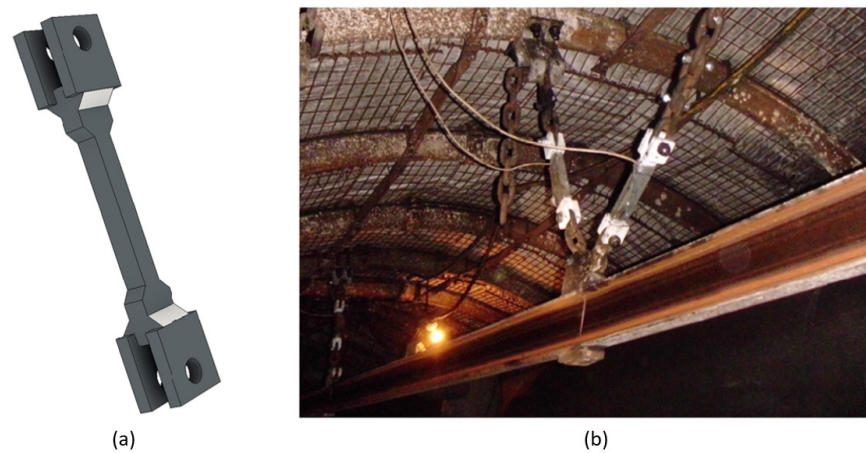

(a)　　　　　　　　　　　　(b)

Figure 1. Model of the force measurement sensor (**a**) and the method of its installation in the suspension of the monorail route (**b**). (Reprinted from Ref. [24]).

Figure 2 shows a view of a 90 m long test track, developed for testing the new design solutions for suspended monorail components, developed in the INESI project.

Figure 2. Overal view of the test track on the test stand (**a**); an operator's view (**b**); the way of mounting of the thermal camera (**c**) [25].

Another test was to measure temperature generated during the emergency braking at the contact point between the surface of the brake block and the rail web of the suspended route (Figure 2c). The measurements were taken on the stand for testing the emergency

braking devices, located in the laboratory of the Central Mining Institute (GIG) [26,27]. The stand consisted of a flywheel, representing the inertial parameters of the moving suspended route, and an emergency braking device. The flywheel was accelerated to the speed corresponding to the assumed linear speed of the monorail (max. 5.7 ms^{-1}) by equalizing the circumferential speed of the wheel with the travel speed of the monorail. Then, the wheel was stopped by clamping the brake shoes pressing the brake pads on it. The temperature was measured using the thermocouples (measuring the temperature inside the brake shoe) and using a thermal imaging camera (measuring the temperature on the surface of the actuators).

2.2. Creation of the Computational Model

Under the conditions of an operating mining plant, testing is associated with difficulties in transport, necessary for the normal operation of the mine, which limits the possibility of creating variants. It is not permissible to reconstruct the method of suspending and stabilizing the route of the suspended monorail. Another technical limitation is the number of sensors that can be installed along the monorail route. For this reason, a numerical model of the suspended monorail was created. The model corresponded to suspended monorail moving on the test track to enable its validation. The second reason for choosing this unit was the installation of innovative solutions, unavailable in other drivetrains. In addition, there is more flexibility on the test stand regarding the suspended monorail test plan (speed, number of active brakes, etc.). The computational model was created in ADAMS software, an environment for the analysis of kinematics and dynamics of multi-body systems (MBS). This type of software allows to calculate forces, torques, and reaction at certain points (e.g., fixation, joint, contact area). Additionally, there is an opportunity to calculate and observe the value of velocity, accelerations, and vibrations related to every part or assembly of the model. Using the co-simulation technique, there are possibilities to combine the Adams software with other software (e.g., Matlab/SIMULINK). This presents the opportunity to test the control system related to the MBS model. The developed computational model corresponded to the transport unit and consisted of rigid bodies representing a modified Becker-Warkop KP-95 locomotive (operator's cabin, a machinery part, two gear drives integrated with multi-plate brakes), a passengers' cabin, and an emergency braking device, equipped with two pairs of brake pads, as shown in Figure 3. In addition, the computational model defines the connections between these bodies, the parameters of contacts between the interacting bodies, as well as the vectors of active forces and moments.
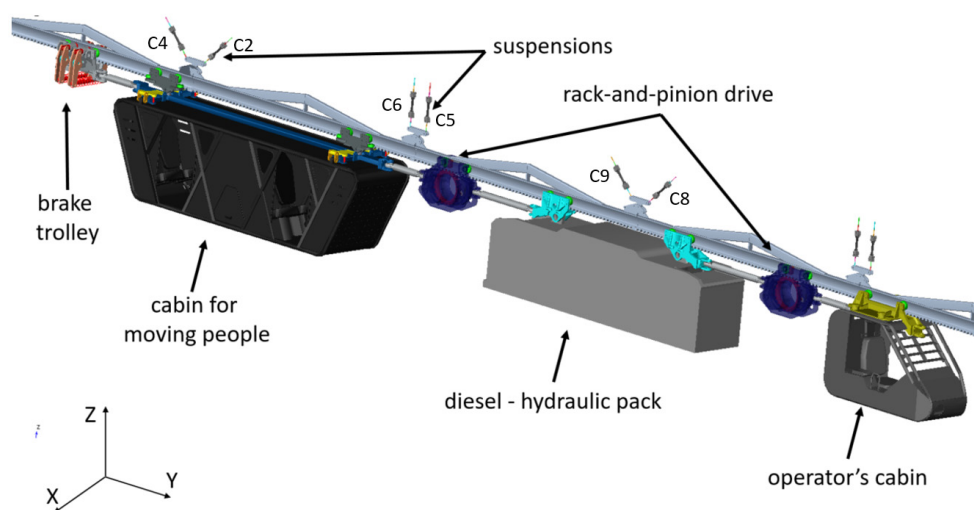

Figure 3. Computational model of a monorail suspended on a test track [25].

Presented numerical model was the base version of the calculation model and it was validated.

2.3. Validation of the Computational Model

Simulation of the travel and braking of the suspended monorail with boundary conditions corresponding to the conditions on the test stand was the base to validate the numerical model. The speed of the monorail at which the braking starts and the braking force were included as the boundary conditions. For validation of the computational model, emergency braking was carried out on the test stand as follows:

- with the use of one pair of pads in the brake device, from the speed of 3 ms^{-1},
- with the use of one pair of pads in the brake device, from the speed of 5 ms^{-1},
- with the use of two pairs of pads in the brake device, from the speed of 5 ms^{-1}.

Contact parameters describing the interaction between the rigid bodies in the computational model were the main variable during adjusting the computational model. The contact parameters adopted in the model are described in [28].

One of the comparable parameters that was measured and calculated on the test stand using the provided model was maximum deceleration during emergency braking. Table 1 shows the maximum deceleration recorded during stand testing and those determined through numerical simulations using the initial and final contact parameters.

Table 1. Maximum deceleration and results of matching the computational model to the real object (Adapted from Ref. [28]).

	Maximum Deceleration at the Initial Contact Parameters (ms^{-2})/Difference with Reference to Stand Tests, %	Maximum Deceleration with Final Contact Parameters, ms^{-2}/Difference with Reference to Stand Tests, %	The Test Stand's Average Maximum Deceleration	Model of Adjustment after Modification of the Contact Parameters
V = 3 ms^{-1}, braking with one pair of pads	3.7/−20.0	4.3/−5.2	4.6	improvement by 14.8%
V = 5 ms^{-1}, braking with one pair of pads	4.1/−19.4	5.6/+9.8	5.1	improvement by 9.6%
V = 5 ms^{-1}, braking with two pairs of pads	5.6/−20.1	7.4/+4.9	7.0	improvement by 15.2%

In addition, Figure 4 shows the acceleration curves recorded on the test stand (three tests were carried out) and those determined by numerical calculations during the simulation of emergency braking with two pairs of shoes at the speed of 5 ms^{-1}.
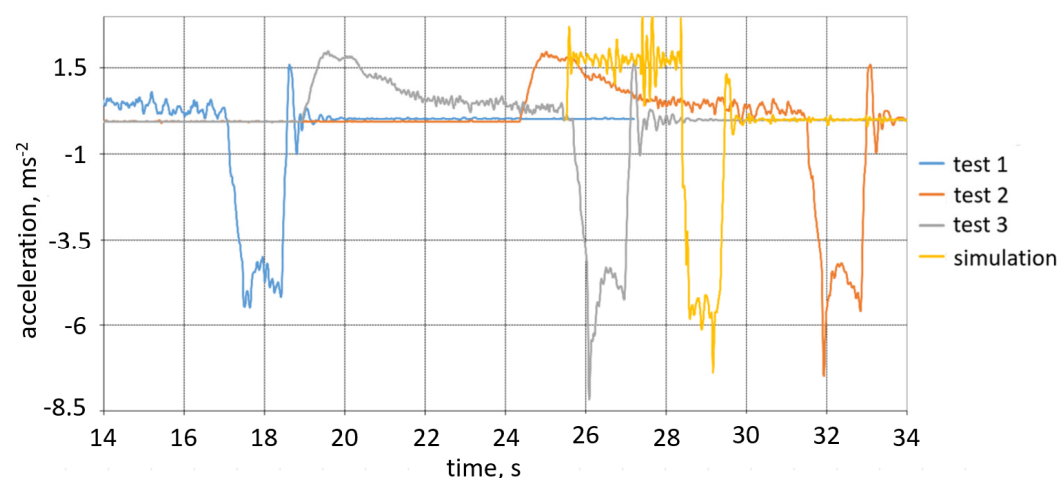

Figure 4. The monorail's accelerations measurement during stand tests and numerical calculations when two pairs of shoes were used to apply emergency brakes from a speed of 5 ms^{-1} (Reprinted from Ref. [28]).

Other parameters analyzed during computational model verification were the forces in the suspensions of the monorail route. Figure 5 presents maximum forces measured in the vertical (C5 and C6) and diagonal (C2 and C4 or C8 and C9) suspensions during travel at the speed of 3 ms^{-1} and 5 ms^{-1}.
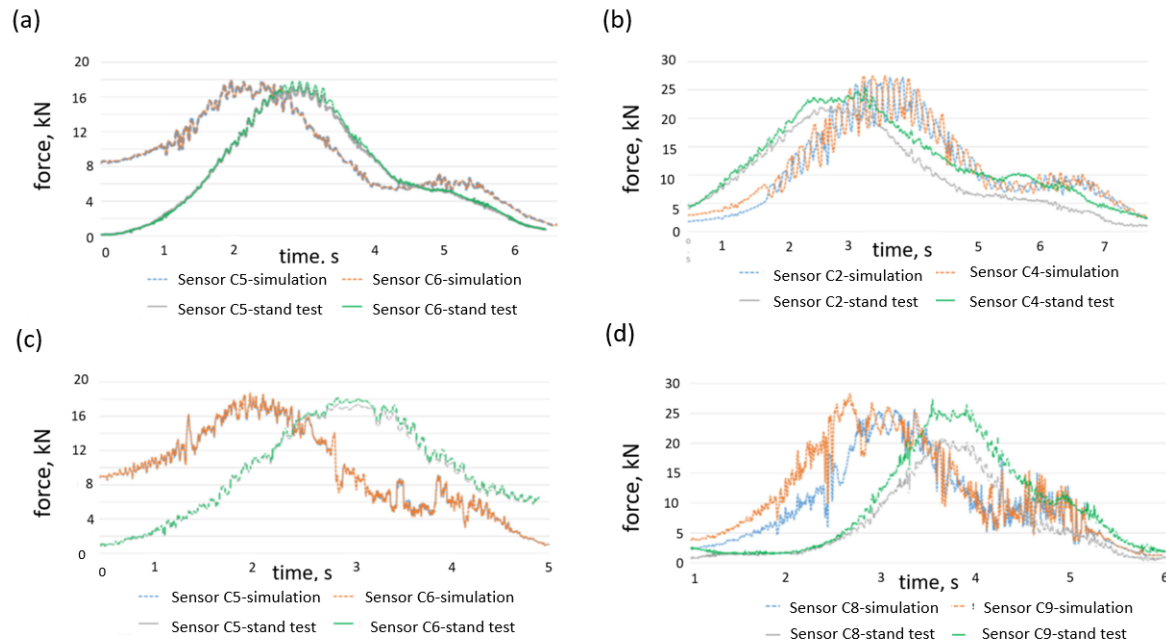
(a)

(b)

(c)

(d)

Figure 5. Loads in the suspensions: (**a**) vertical direction at the travel speed 3 ms^{-1}, (**b**) diagonal direction at the travel speed 3 ms^{-1}, (**c**) vertical direction at the travel speed 5 ms^{-1}, (**d**) diagonal direction at the travel speed 5 ms^{-1} (Adapted from Ref. [29]).

In addition, Table 2 presents maximum forces recorded in selected suspensions during travel at the speed of 3 ms^{-1} and 5 ms^{-1} on the test stand and calculated during the simulation.

Table 2. Maximum forces (F_{max}) in the suspensions during the travel of monorail (Adapted from Ref. [29].

	Calculated in Simulation, kN	Measured on the Test Stand, kN	Difference Calculated in Relation to the Measured Value, %
	Travel speed 3 ms^{-1}		
F_{max} in C5 (vertical)	17.97	17.3	3.84
F_{max} in C6 (vertical)	17.93	17.78	0.87
F_{max} in C2 (diagonal)	27.2	22.25	22.3
F_{max} in C4 (diagonal)	27.49	25.27	8.79
	Travel speed 5 ms^{-1}		
F_{max} in C5 (vertical)	18.66	17.42	7.13
F_{max} in C6 (vertical)	18.71	18.14	3.18
F_{max} in C8 (diagonal)	25.71	20.75	23.9
F_{max} in C9 (diagonal)	28.27	27.29	3.57

Based on the comparisons of suspended monorail decelerations and forces in the route suspensions, it was found that the computational model allows for further numerical simulations, going beyond the scope of stand tests. These include changing the parameters

and the method of emergency braking as well as changing the method of suspension and stabilization of the suspended monorail route.

2.4. Expansion of the Computational Model

The computational model was extended by adding a control module for extended analyses, based on the results of numerical simulations. The module was developed in the Matlab/Simulink software environment. This way, by using the co-simulation technique, the possibility of controlling the model was introduced, mainly in relation to the braking method and the braking force (change in the braking force, change in the time for the braking force to reach the maximum value, etc.), or setting the boundary conditions, such as the maximum speed of the monorail travel, or the possibility of activating or deactivating each force vector and moment. The extended computational model is shown in Figure 6.
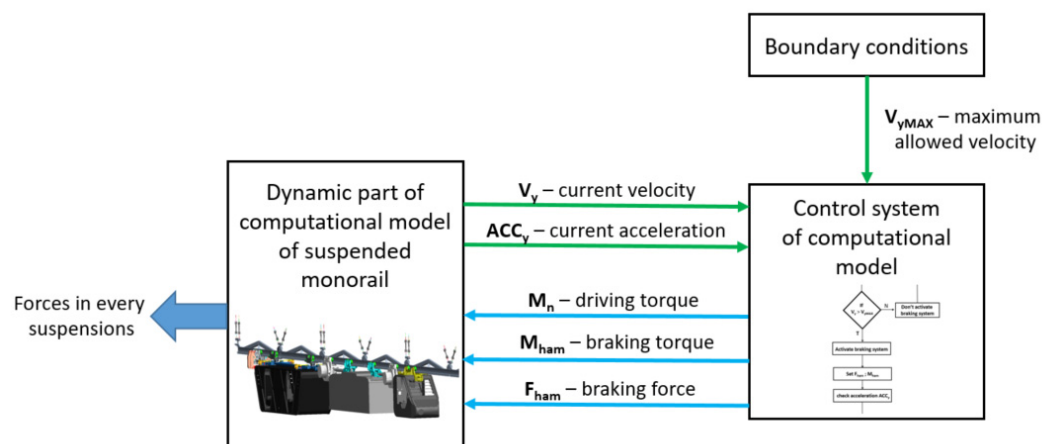

Figure 6. Diagram of extended numerical model (Adapted from Ref. [29]).

The second modification, giving great opportunities for the analysis of emergency braking, was the variant of suspension and stabilization of the monorail route. This variant consisted in modifying the position of each suspension in relation to the route (vertical, diagonal) and introduction of stabilizing side lashings. In total, an emergency braking was simulated for seven variants of the suspending method. All variants of the method for suspending and stabilizing the route are presented below:

- Variant 1: The rails were suspended on straight suspensions that were parallel to the route of the monorail.
- Variant 2: This variant is an extension of the variant 1 by adding two side lashings to rail No. 2. The length of the lashings was fixed, and they were tilted from the horizontal upwards by an angle of $10°$.
- Variant 3: This variant is an extension of the variant 2, adding the flexibility of the side lashing. This was done by introducing an elastic-damping component, enabling the lashings to be extended during the impact of an external force. The modulus of elasticity in relation to the side lashings was $6.66 \times 10^6 \, \mathrm{Nm}^{-1}$.
- Variant 4: Additional side lashings were added to the computational model of the suspended route, installed on rails 10 and 22. As with the earlier variations, the lashings were installed in the same manner (articulation from the horizontal by an angle of $10°$).
- Variant 5: This variant is an extension of the variant 4, adding the flexibility of the side lashing. Elastic components with the same properties as in variant 3 were used.
- Variant 6: Alternating straight suspensions (perpendicular to the rails) and diagonal suspensions were introduced to the computational model. The diagonal suspensions were inclined at an angle of $45°$; one in the direction of travel and the other in the opposite direction. This way of creating the route was used on the test track as part of the INESI project.

- Variant 7: All rail suspensions of the computational model were inclined (45°) in relation to the route of the monorail. Each pair of suspensions was inclined in the direction and opposite direction of the monorail movement [30].

Modifications introduced to the computational model enabled extended simulations and an in-depth analysis of the impact of the variation of the travel speed on the safety and comfort of the personnel as well as on the safety of the mine infrastructure.

3. Impact of Increasing the Speed of Travel of Suspended Monorail on Its Dynamic Parameters

On the basis of the real tests and numerical simulations, as well as the analysis of the results, the impact of increasing the permissible speed of the suspended monorail on the safety of people and the roadway infrastructure was assessed, especially regarding the emergency braking. The time process of the deceleration acting on a person in the transport unit, the impact of speed on the route suspensions' loads, and changes in the surface temperature of the brake pads were assessed. The synthesis of the analyses is presented in the following sections of the article.

3.1. Impact of Increasing the Travel Speed on Decelerations Acting on the Users

The following numerical simulations of emergency braking were performed to examine how variations in speed would affect decelerations experienced by the monorail's users:

- on a horizontal route (3 ms^{-1} and 5 ms^{-1}),
- downward with an inclination of 30° (3 ms^{-1} and 5 ms^{-1}),
- on a horizontal track, with two pairs of pads and two multi-disc brakes (5 ms^{-1}).

In addition, in the simulations, 1 or 2 pairs of brake shoes were used for emergency braking and the multi-disc brake was activated or deactivated. During the simulation in which the multi-disc brakes were activated, a delay time of 0.3 s and 0.1 s was defined regarding the maximum braking forces. Table 3 presents a list of boundary conditions and the simulation results, such as maximum deceleration during braking, maximum speed, braking time, braking distance.

Table 3. Results of numerical symulations during emergency braking of a suspended monorail (Reprinted from Ref. [28]).

Boundary Conditions				Results of Numerical Simulations			
Assumed Speed at Which Emergency Braking Starts, ms^{-1}	Route Inclination, °	Number of Activated Brake Shoes	Number of Multi-Disc brakes Activated/Activation Delay Time, s	Maximum Deceleration during Braking, ms^{-2}	Maximum Speed Reached by the Monorail, ms^{-1}	Braking Time, s	Braking Distance, m
3	0	1	0	4.3	3.0	1.2	1.90
5	0	1	0	5.6	5.0	1.8	4.58
5	0	2	0	8.6	5.0	1.1	3.54
5	0	2	2/0.1	17.6	5.0	0.7	2.05
3	30	2	1/0.3	8.3	3.5	1.1	2.68
3	30	2	1/0.1	8.3	3.5	0.9	2.14
5	30	2	1/0.3	16.8	5.6	1.8	5.58
5	30	2	1/0.1	13.5	5.5	1.6	4.29

The analyses showed that, during emergency braking on inclined routes (when driving to the dip), the impact of gravitational movement forces results in extending the braking distance. It was also found that during the activation of too high braking force on a horizontal route, the permissible decelerations affecting people traveling by monorail may be significantly exceeded. On the other hand, the ability to stop the monorail on a route with high inclines is not guaranteed. However, reducing the braking force results in reduced overloading during emergency braking.

3.2. Impact of Increasing the Forces in the Monorail Route Suspensions

An emergency braking of the suspended monorail set with the speed in the range from 1 ms^{-1} to 6 ms^{-1} (every 1 ms^{-1}) was simulated to determine the influence of the travel speed on the forces in the route suspensions. The forces in each suspension of the monorail route were measured during the simulation. The simulations refer to variant 6 of the suspensions arrangement. Figure 7 shows the maximum values of the forces recorded in the suspensions in relation to each travel speed of the transport unit.
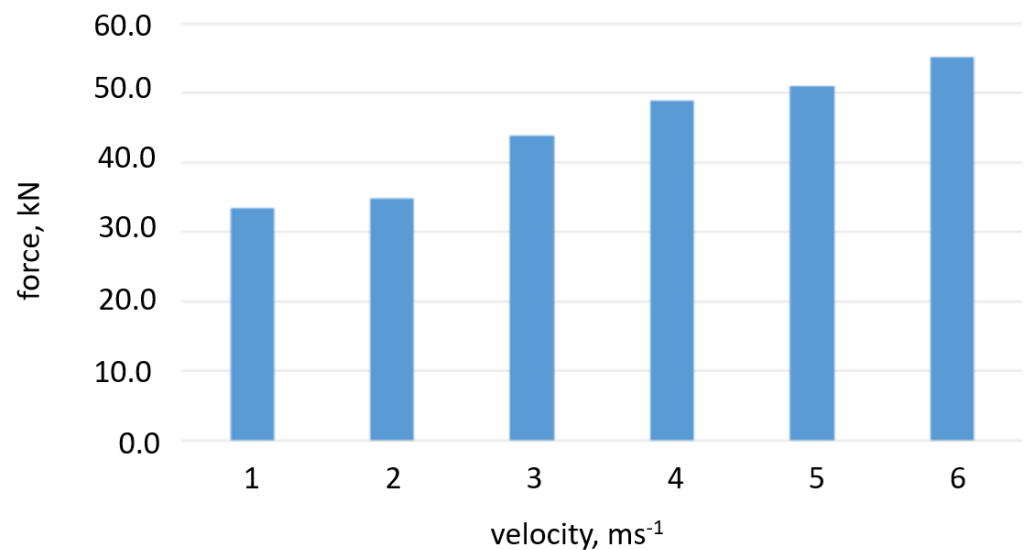
Figure 7. The highest suspension forces corresponding to the maximum travel speed [25].

The diagonal suspensions received the strongest tensions during emergency braking, helping the position of the suspended monorail track. With the increase of the speed at which the emergency braking starts, the dynamic overload recorded in the suspensions increased. In addition, Figure 8 shows the course of the force values in the most heavily loaded suspensions during braking from the given speed.
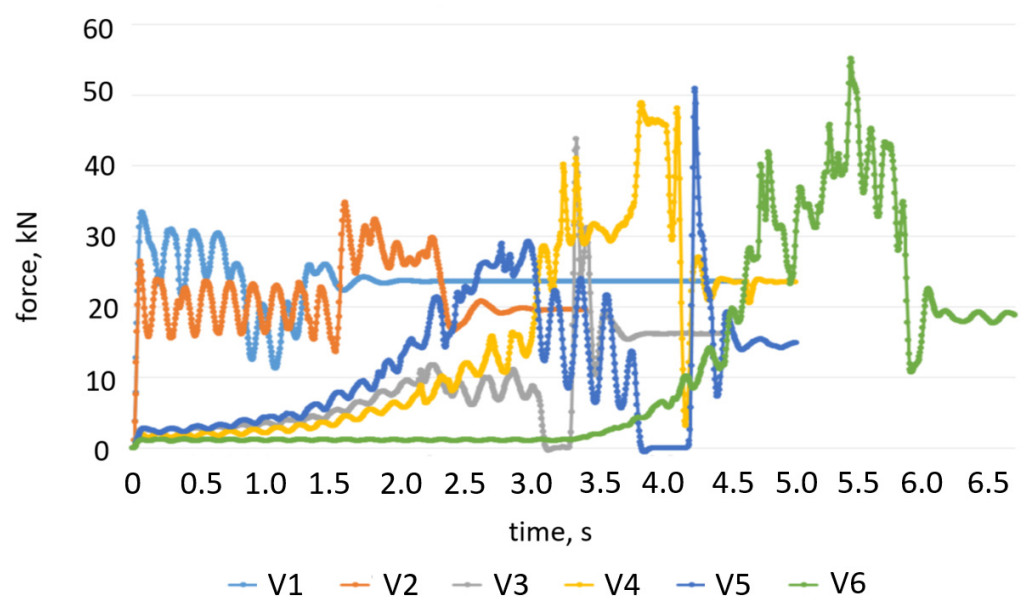

Figure 8. Curve of the force in the most heavily loaded suspensions during emergency braking from different speeds [25].

Based on the results, it was determined how much the force value increased in the most heavily loaded suspension compared to the value recorded at the lowest speed, i.e., 1 ms^{-1} (Table 4), and the maximum speed that was permitted for the suspended monorail when carrying passengers, i.e., 2 ms^{-1} (Table 5). The difference in the value of forces is presented in the form of their increase in Newtons and in the form of a percentage increase in relation to the base value.

Table 4. Increase of the maximal forces corresponding to the forces recorded during emergency braking from the speed of 1 ms^{-1} (Adapted from Ref. [29]).

	Force Increase, N	Percentage Force Increase, %
Base value—maximum force in the suspension during emergency braking from speed 1 ms^{-1}	33,406.63	
Increase of F_{max} at V = 2 ms^{-1}	+1373.32	+4.11
Increase of F_{max} at V = 3 ms^{-1}	+10,421.68	+31.2
Increase of F_{max} at V = 4 ms^{-1}	+15,508.91	+46.42
Increase of F_{max} at V = 5 ms^{-1}	+17,516.7	+52.43
Increase of F_{max} at V = 6 ms^{-1}	+21,811.06	+65.23

Table 5. Increase of the maximal forces corresponding to the forces recorded during emergency braking from the speed of 2 ms^{-1} (Adapted from Ref. [29]).

	Force Increase, N	Percentage Force Increase, %
Base value—maximum force in the suspension during emergency braking from speed 2 ms^{-1}	34,779.95	
Increase of F_{max} at V = 1 ms^{-1}	−1373.32	−3.95
Increase of F_{max} at V = 3 ms^{-1}	+9048.36	+26.020
Increase of F_{max} at V = 4 ms^{-1}	+14,135.59	+40.64
Increase of F_{max} at V = 5 ms^{-1}	+16,143.38	+46.42
Increase of F_{max} at V = 6 ms^{-1}	+20,437.74	+58.76

Emergency braking is the most unfavourable situation from the point of view of dynamic loads on the monorail suspensions. In this situation, the greatest overloads occur, and the analyses indicate that when the maximum speed of the suspended monorail raises, the dynamic overloads recorded in the route joints increase.

One of the causes of dynamic overloads is the fact that the route of the suspended monorail is not a rigid body, and the complete route and the neighbouring rails have the possibility of movement in joints in relation to each other. Therefore, the suspension may loosen temporarily and then dynamically loaded. In addition, increasing the maximum travel speed causes the kinetic energy of the transport unit to increase exponentially.

3.3. Impact of Increasing the Travel Speed on the Brake Pads Temperature during Emergency Braking

Emergency braking from the speed of 3 ms^{-1} and 5 ms^{-1} with one or two pairs of brake pads was tested. The tests were carried out on the Central Mining Institute test stand. Figure 9 presents the temperature curve of a pair of brake shoes during the braking test from the speed of 3 ms^{-1} and 5 ms^{-1}. For each variant, 5 measurements were carried out.
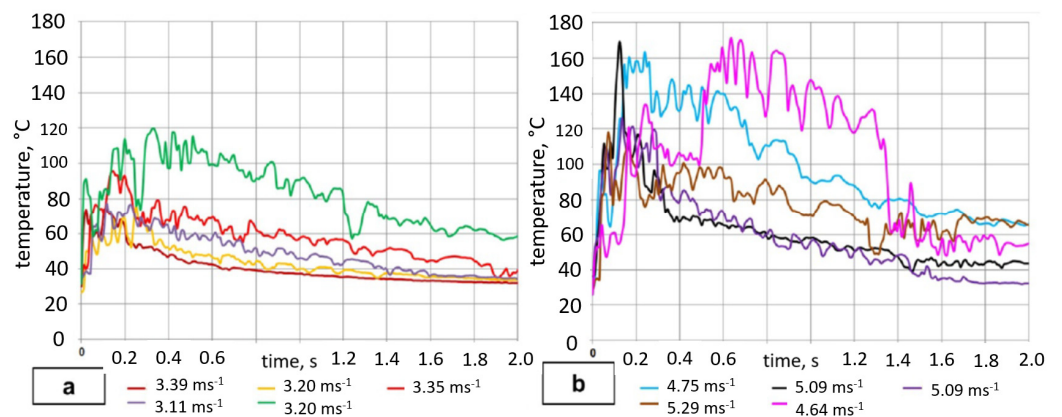
Figure 9. Brake pad temperature T at the speed (**a**) 3 ms^{-1}, (**b**) 5 ms^{-1} (Adapted from Ref. [27]).

Then, the results were analysed, and the maximum temperatures recorded for each pair of jaws were presented. The maximum temperature recorded during braking with the front (right) pair of brake shoes was 132.0 °C for the speed of 3 ms^{-1} and 154.4 °C for the speed of 5 ms^{-1}. A similar situation occurred in the case of the rear (left) pair of brake shoes, where the maximum temperature recorded during braking from 3 ms^{-1} was 119.4 °C and during braking from 5 ms^{-1} it was 171.3 °C. Mechanical sparking was observed on thermal images during emergency braking. Due to the method of installation and the location of the thermal imaging camera, this phenomenon is best visible in the images showing braking with the left pair of brake shoes. Figure 10 shows photos from a thermal imaging camera in relation to emergency braking at the speed of 3 ms^{-1} using the right, left and both pairs of brake shoes. On the other hand, Figure 11 shows analogous values for the speed of 5 ms^{-1}. The figures contain a legend which shows the range set for optimal viewing and interpretation of the nature of the phenomenon. The highest temperatures were marked with an indicator located in the place of its occurrence. In the case of using the legend range covering the highest measured values, the thermogram would be unreadable.

As can be seen in the images, the increase in speed at which emergency braking starts results in an increase in the brake shoes temperature and intensification of mechanical sparking. It is also worth noting that increasing the surface of the brake shoes (by using two pairs of brake shoes instead of one pair) enables reducing the recorded temperature during emergency braking.
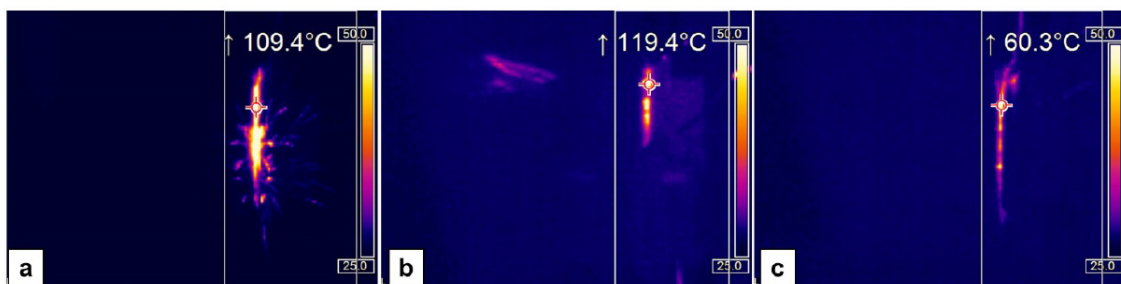

Figure 10. Maximum temperatures of braking pads at kinematic energy E_k = 2258 J (v = 3 ms^{-1}): (**a**) for the left pair L; (**b**) for right pair R; (**c**) for both the brake pads pairs L+R. The legend is given in degrees Celsius (Reprinted from Ref. [27]).
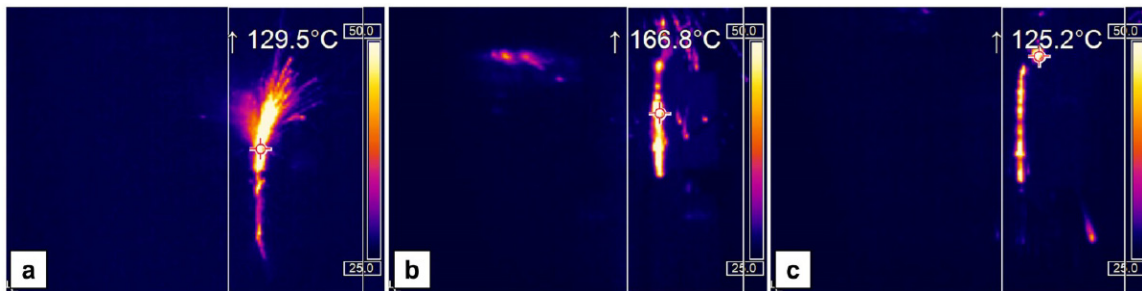
Figure 11. Maximum temperatures of braking pads at kinematic energy E_k = 6273 J (v = 5 ms^{-1}): (**a**) for the left pair L; (**b**) for right pair R; (**c**) for both the brake pads pairs L+R. The legend is given in degrees Celsius (Reprinted from Ref. [27]).

4. Proposed Solutions Improving the Safety and Increasing the Travel Comfort, as well as Guidelines for Safe Travelling at Higher Speeds

Based on the results of the analyses, it was found that during emergency braking from a higher driving speed, the maximum permissible decelerations affecting a person in the transport unit (operator or passengers) may be exceeded. Maximum permissible forces acting on each suspension of the route may also be exceeded. Therefore, concepts of the solutions to increasing the level of safety and comfort of using this means of transport have been suggested. The proposed concepts of changes were implemented in the computational model of the suspended monorail and numerical simulations enabled assessing how the proposed solutions affect dynamic quantities, including the ergonomic assessment of the proposed design solutions.

4.1. Analysis of the Method for Stabilization of the Fast Monorail Route

To be able to travel at a higher speed, the suspended monorail requires proper installation and stabilization of the route. To assess the impact of the superstructure on the dynamic parameters of the suspended monorail, emergency braking was simulated for the speed of 5 ms^{-1} with 7 different variants of suspension and stabilization of the monorail route (see Section 2.4. Expansion of the computational model). Each simulation had the following procedure: acceleration of the transport unit to the speed of 5 ms^{-1}, travelling at this speed for 1 s, and then emergency braking with two pairs of brake shoes. During the simulation, the time process of acceleration of the transport unit, forces in the route suspensions, and displacements of the rails of the route were recorded. Figure 12 presents the maximum and minimum accelerations for each variant.
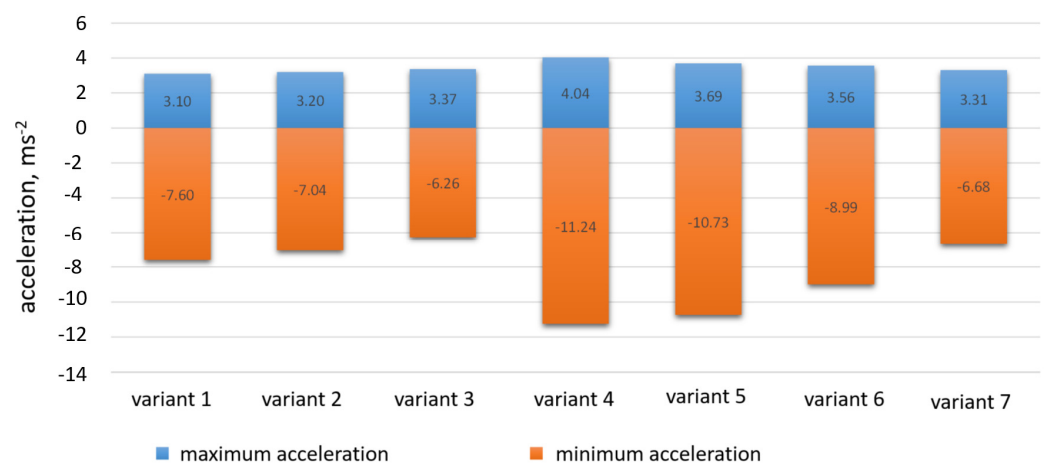

Figure 12. Extreme accelerations of the suspended monorail transport unit for each variant (Reprinted from Ref. [30]).

Maximum resultant forces recorded in the selected suspensions of the route (marked as cz11—cz22) are given in Table 6. The symbols cz11—cz22 correspond to lashings next to each other in each of the seven variants.

Table 6. Maximum resultant forces recorded in the suspensions 11–22 (Adapted from Ref. [30]).

Variant No.	Maximum Resultant Force											
	cz11, N	cz12, N	cz13, N	cz14, N	cz15, N	cz16, N	cz17, N	cz18, N	cz19, N	cz20, N	cz21, N	cz22, N
1.	22,052	25,741	25,015	23,675	31,789	24,582	21,596	18,553	7384	6079	1619	1069
2.	22,227	24,496	25,312	24,801	30,205	23,031	17,607	18,622	7164	6816	1555	1377
3.	24,519	24,156	23,947	23,188	23,055	19,035	16,939	18,035	6306	5980	1474	1050
4.	19,222	20,777	19,905	19,830	26,445	21,541	16,879	17,728	6778	8171	5339	2648
5.	21,733	23,721	25,812	25,048	27,732	27,118	16,996	18,059	5784	6122	2031	4346
6.	23,998	34,444	23,496	23,471	47,472	29,085	17,363	17,316	11,932	9786	1028	1014
7.	28,042	26,823	29,308	26,103	39,600	24,043	27,935	26,671	9744	8837	1839	1471

The presented results were divided into the following groups in relation to the criterion of the permissible load to the suspensions and arches of the roadway roof support:

- Group I: The resultant forces in the suspensions do not exceed 10 kN. The group of these suspensions in the table is marked in green. This means that they are at a low level (safe values).
- Group II: The resultant forces in suspensions are greater than 10 kN, but less than 30 kN. This group is marked in yellow and orange in the table. Loads at this level are higher than in group I. However, they do not exceed the permissible values and should not cause dangerous situations.
- Group III: The resultant forces in suspensions exceed 30 kN. This group is marked in red in the table. These are the most loaded suspensions. In this group, suspensions should be monitored as limit values may be exceeded. This may result in dangerous situations.

Displacement of the rails (first and tenth rail) was another recorded parameter. Table 7 presents the maximum displacements in the Y axis (in the direction of travel) and in the Z axis (vertical axis), in relation to the analysed variants of the route suspension method. The results are presented for rails 1 and 10, which in the selected variants were additionally protected by stabilizing lashings. Schemes with descriptions of the suspended route for each variant are presented in [30].

Table 7. Maximum route displacement (rails No. 1 and 10) in each variant of the route suspension (Adapted from Ref. [30]).

Variant No.	Maximum Displacement of Rail 1			Maximum Displacement of Rail 10		
	In Y axis, m	In Z axis, m	In X axis, m	In Y axis, m	In Z axis, m	In X axis, m
1.	0.365	0.132	0.005	0.365	0.132	0.001
2.	0.133	0.084	0.001	0.129	0.017	0.001
3.	0.188	0.078	0.001	0.184	0.03	0.001
4.	0.111	0.079	0.001	0.104	0.107	0.0002
5.	0.157	0.075	0.002	0.15	0.114	0.0003
6.	0.009	0.002	0.004	0.009	0.002	0.001
7.	0.005	0.001	0.002	0.005	0.001	0.002

The largest displacements occurred in relation to the route installed according to variant 1 (without stabilization). Maximum values indicate route destabilization, which in practical terms would not be acceptable. Adding one yielding lashing results in a decrease by approximately 50% and adding two or more by approximately 60%. While emergency braking, displacements of about 180 mm decrease the maximum force in the stabilizing lashings without harming the crew or passengers.

Unfavourable phenomena include excessive movement of the route, observed in variant 1. Stiffening of the route is unfavourable because it results the occurrence of high forces in the lashings of the route (variants 6 and 7) and creates excessive force in a load on the roadway support frame that is more than what is permitted. The presented method of analysis enables the optimization of the method of suspending the monorail route in terms of minimizing the loads to the suspensions and the route stabilization. Numerical simulations should be a permanent practice in the designing process, in particular with regard to sections of routes intended for high-speed suspended railways used for the people movement.

On the basis of the analysis results, it was found that the proper suspension method and stabilization of the suspended monorail route is of key importance in the aspect of safe passenger transport by suspended monorail with the travel speed increased to $5\,\text{ms}^{-1}$. Insufficient stabilization of the route results in its excessive displacement. This phenomenon is unfavourable and can cause dangerous situations, such as breaking the suspension chain or collision of subassemblies of the monorail set with the rest of the mine infrastructure. Excessive displacement of the route was observed during braking in variant 1.

In order to stabilize the route movement, especially in the axis in line with the direction of the monorail travel, it is important to introduce side stabilizing lashings. However, making them more flexible is an effective way to reduce the maximum forces acting on these lashings during the emergency braking. Such a situation is observed in variants 2 and 3, especially with regard to the force component in the direction of the monorail travel.

As a result of the analysis of variants of the suspended monorail route, it was found that:

- due to the criterion of minimizing the overloads affecting the operator and the crew, it is most advantageous to use variants 3 and 7;
- due to the criterion of minimizing the forces in suspensions of the monorail route, it is most advantageous to use variant 3 or;
- due to the criterion of minimizing the forces in the side stabilizing lashings it is best to use variant 4 or 5.

Thus, according to the analyses, each case of designing the route and the method of its suspension and stabilization should be considered individually, taking into account, among others, such data as: the condition of the roadway support at the route construction place, the configuration of the most frequently used transportation unit on a given route, and the type of transport system and the expected frequency of crew movement at increased speed. In the process of designing and analysing the method of suspension and stabilization, the use of numerical simulation techniques can be an effective tool supporting the designers.

4.2. Sequential Emergency Braking Concept and Braking Algorithm

According to Polish law, the suspended monorail assembly must be secured with brake trolleys or other emergency braking devices with a static braking reliability factor of at least 1.5 in relation to the maximum rolling force of the transport set [31]. In accordance with Polish law, proprietary drives of suspended monorails, intended for use in inclined workings with an inclination of not more than $45°$, must have a braking reliability factor, determined as the ratio of the maximum braking force to the maximum traction force of the own drive, not less than 1.5, requiring the braking deceleration of the transport set to be not less than $1\,\text{ms}^{-2}$ and not more than $10\,\text{ms}^{-2}$ [8]. These requirements ensure that a fully loaded transport unit can be effectively stopped at the maximum inclination at which such a transport unit can move. However, in a situation where the transport unit, after unloading, will return unloaded, additionally driving along a horizontal route or on an incline with the maximum permissible speed, it is very likely that the maximum permissible deceleration affecting the monorail operator, i.e., $10\,\text{ms}^{-2}$, will be exceeded. This is a dangerous situation that could lead to an accident. Considering this problem, KOMAG developed the concept of an innovative, sequential method of braking the suspended monorail, in which the maximum braking force securing the transport unit is maintained. However, it is divided

into two braking devices (or, with higher forces, two groups of devices), e.g., a friction brake and a multi-plate brake. In emergency braking, the first braking stage is activated, e.g., a friction brake. Then, the monorail deceleration is monitored and, depending on its value, a decision is made to activate or not activate the second stage of braking. This sequential braking enables adapting the braking force to the current conditions in which the monorail operates (route inclination, mass of the unit and load, etc.). In order to properly control the sequential braking system, a dedicated algorithm has been developed. In this algorithm, the following parameters are set: the limit braking deceleration, which determines the activation of the second stage of braking, and the time of activation of the second stage of the braking system. The block diagram of the sequential emergency braking algorithm (area surrounded by a green line) together with the part responsible for controlling the numerical simulation (area surrounded by a red line) is shown in Figure 13.
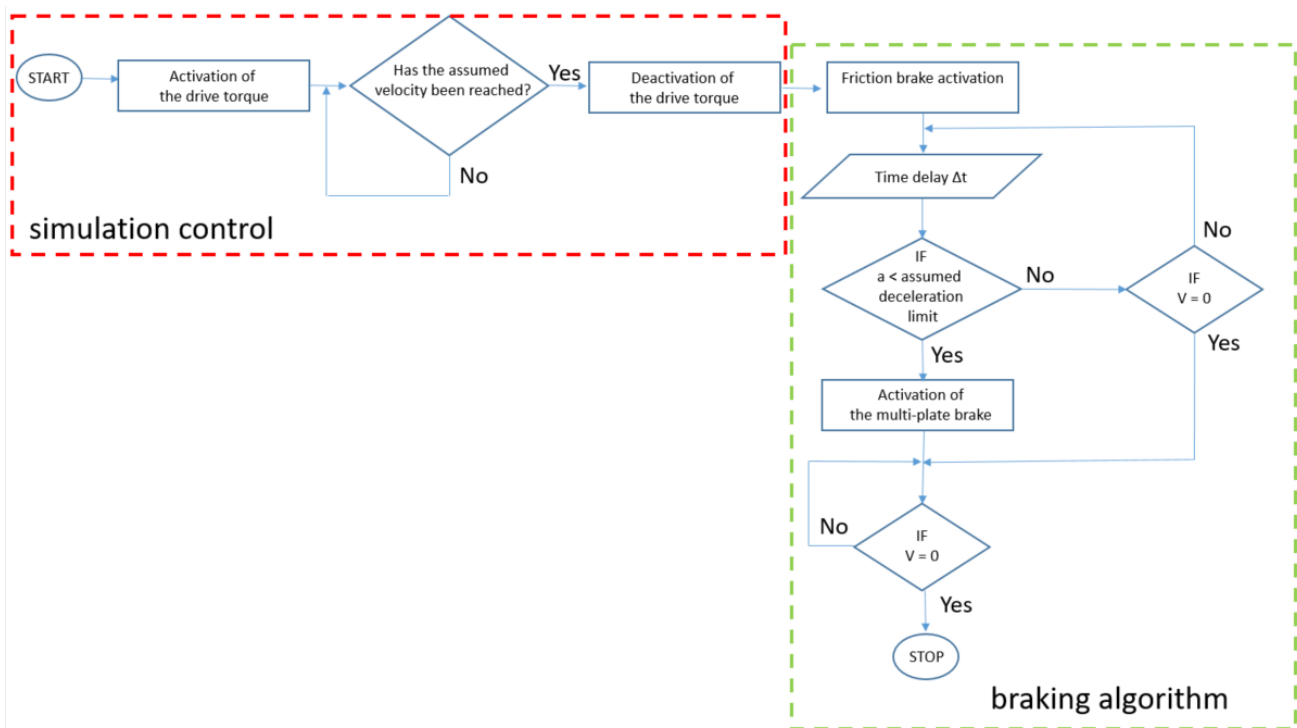

Figure 13. Algorithm of the emergency braking simulation sequence (Reprinted from Ref. [32]).

A detailed description of the operation of the sequential braking algorithm is presented in [32]. A number of numerical simulations were carried out covering the emergency braking process from speeds of 3 ms^{-1} and 5 ms^{-1}, on a horizontal route and on a dip with inclination of 30°, using three different settings of the second stage activation threshold and three values of the second stage activation time delay. In addition, the reduction of the first stage braking force was also taken into account in the simulations. The parameters settings and simulation results of emergency braking from the speed of 3 ms^{-1} on a horizontal route are presented in Table 8.

Table 8. Simulation results of emergency braking from the speed of 3 ms^{-1}, on not inclined route, with different settings of the braking algorithm (Reprinted from Ref. [32]).

Threshold Braking Deceleration, ms^{-2}	Second Stage Activation Time Delay, s	Activation of the Second Stage of Braking	Maximum Deceleration of Braking, ms^{-2}	Maximum Deceleration of the First Stage of Braking, ms^{-2}	Braking Time, s	Braking Distance, m
4	0.1	No	4.34	———	1.18	1.90
4	0.3	No	4.30	———	1.18	1.92
4	0.5	No	4.34	———	1.18	1.93
5	0.1	Yes	9.23	4.34	0.73	1.33
5	0.3	Yes	9.11	4.34	0.88	1.60
5	0.5	Yes	9.12	4.34	0.99	1.79
6	0.1	Yes	9.01	4.34	0.73	1.32
6	0.3	Yes	8.83	4.34	0.87	1.60
6	0.5	Yes	8.89	4.34	0.99	1.79

Parameters settings and simulation results of emergency braking from the speed of 5 ms^{-1}, on a route without inclination, with different settings of the braking algorithm, is presented in Table 9.

Table 9. Simulation results of emergency braking from the speed of 5 ms^{-1}, on not inclined route, with different settings of the braking algorithm (Reprinted from Ref. [32]).

Threshold Braking Deceleration, ms^{-2}	Second Stage Activation Time Delay, s	Activation of the Second Stage of Braking	Maximum Deceleration of Braking, ms^{-2}	Maximum Deceleration of the First Stage of Braking, ms^{-2}	Braking Time, s	Braking Distance, m
4	0.1	No	4.53	———	1.84	4.71
4	0.3	No	4.40	———	1.85	4.72
4	0.5	No	4.35	———	1.85	4.76
5	0.1	Yes	9.10	3.14	0.92	2.78
5	0.3	Yes	9.66	3.66	1.17	3.30
5	0.5	Yes	8.55	3.65	1.17	3.73
6	0.1	Yes	9.84	3.51	0.86	2.75
6	0.3	Yes	9.76	3.62	1.16	3.26
6	0.5	Yes	8.57	3.65	1.17	3.72

Parameter settings and simulation results of emergency braking from the speed of 3 ms^{-1}, on a route to the dip on inclination 30°, with different settings of the braking algorithm, are presented in Table 10.

Table 10. Simulation results of emergency braking from the speed of 3 ms^{-1}, on a route to the dip on inclination 30°, with different settings of the braking algorithm (Reprinted from Ref. [32]).

Threshold Braking Deceleration, ms^{-2}	Delay in Activation of the Second Sage of Braking, s	Activation of the Second Sage of Braking	Maximum Deceleration of Braking, ms^{-2}	Maximum Deceleration of the First Stage of Braking, ms^{-2}	Braking Time, s	Braking Distance, m
4	0.1	Yes	8.56	0.87	0.95	2.15
4	0.3	Yes	8.84	2.498	1.22	2.76
4	0.5	Yes	9.45	3.57	1.24	3.2
5	0.1	Yes	8.35	0.87	0.94	2.15
5	0.3	Yes	8.28	1.60	1.12	2.68
5	0.5	Yes	8.48	1.65	1.25	3.2
6	0.1	Yes	8.35	0.87	0.94	2.1
6	0.3	Yes	8.28	1.60	1.12	2.68
6	0.5	Yes	9.45	3.57	1.24	3.08

Parameter settings and simulation results of emergency braking from the speed of 5 ms^{-1}, on a route to the dip on inclination 30°, with different settings of the braking algorithm, are presented in Table 11.

Table 11. Simulation results of emergency braking from the speed of 5 ms^{-1}, on a route to the dip on inclination 30°, with different settings of the braking algorithm (Reprinted from Ref. [32]).

Threshold Braking Deceleration, ms^{-2}	Delay in Activation of the Second Sage of Braking, s	Activation of the Second Stage of Braking	Maximum Deceleration of Braking ms^{-2}	Maximum Deceleration of the First Stage of Braking ms^{-2}	Braking Time, s	Braking Distance, m
4	0.1	Yes	13.96	3.25	1.62	4.32
4	0.3	Yes	14.23	3.43	1.72	5.15
4	0.5	Yes	10.87	3.43	1.61	6.12
5	0.1	Yes	13.53	2.86	1.61	4.29
5	0.3	Yes	16.84	4.09	1.77	5.58
5	0.5	Yes	10.87	3.29	1.61	5.93
6	0.1	Yes	14.48	3.43	1.57	4.38
6	0.3	Yes	14.89	3.43	1.73	5.14
6	0.5	Yes	10.95	3.45	1.61	6.08

Figures 14–16 display the braking distance at various first stage braking threshold values, the delay in the second stage braking activation, the speed at which the transportation set was stopped, and the route inclination angles.
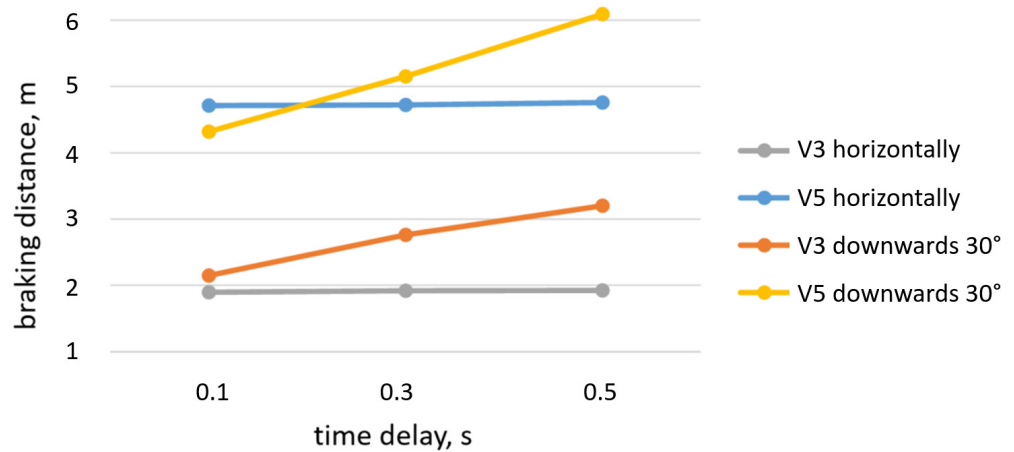
Figure 14. Braking distance in relation to threshold deceleration equal to 4 ms^{-2} (Reprinted from Ref. [32]).
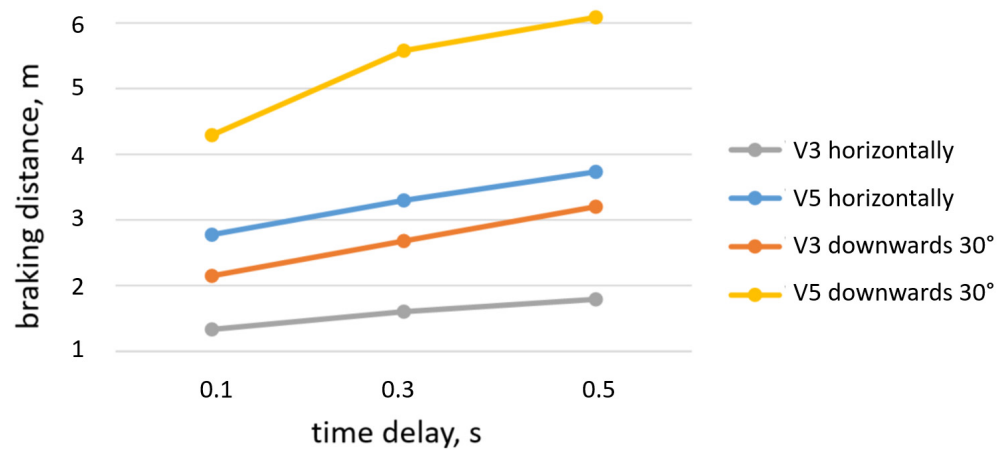

Figure 15. Braking distance in relation to threshold deceleration equal to 5 ms^{-2} (Reprinted from Ref. [32]).
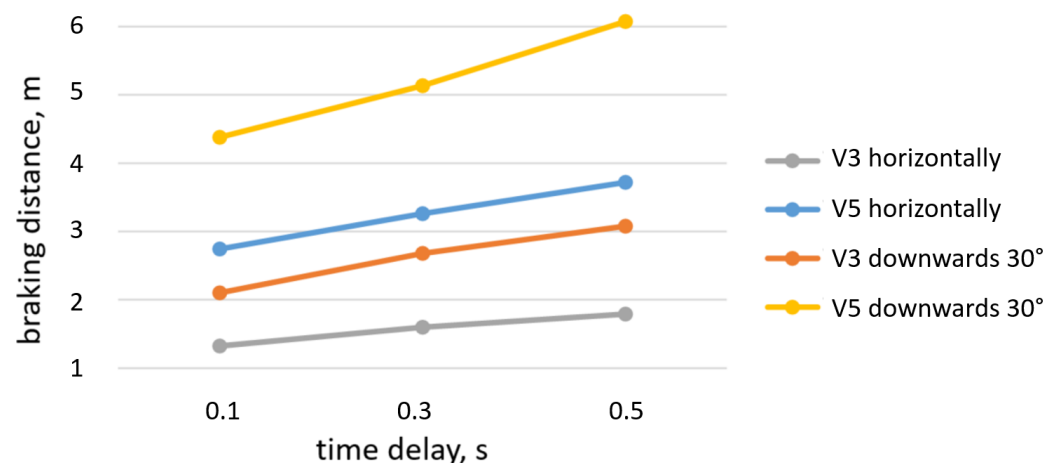

Figure 16. Braking distance in relation to threshold deceleration equal to 6 ms^{-2} (Reprinted from Ref. [32]).

In subsequent simulations, the first-stage braking force was reduced from 12,500 N, by 50% (to 6250 N) and by 75% (to 3125 N). The second stage of braking was activated with a time delay of 0.5 s. In addition, with regard to the reduced braking force (by 50% and 25%), simulations were carried out with a second-stage activation time delay of 1 s. All

tests were carried out with braking from the speed of 5 ms^{-1}. Table 12 presents results of the simulation.

Table 12. The simulation results of the emergency braking, with the reduced braking force at the first stage (Reprinted from Ref. [32]).

Force Pressing the Brake Shoe to a Rail, N	Number of Active Pairs of Brake Shoes	Threshold Deceleration, ms^{-2}	Delay in Activation of the Second Sage of Braking, s	Activation of the Second Sage of Braking	Maximum Deceleration, ms^{-2}	Maximum Deceleration at the First Stage of Braking, ms^{-2}	Braking Time, s	Braking Distance, m
12,500	1	6	0.5	Yes	8.57	3.65	1.17	3.72
6250	1	6	0.5	Yes	7.74	2.07	1.39	4.74
3125	1	6	0.5	Yes	8.68	1.69	1.58	5.34
6250	1	6	1	Yes	8.53	2.44	1.86	6.30
3125	1	6	1	Yes	7.45	2.32	2.05	7.35
12,500	2	6	0.5	No	7.35	———	1.0	2.84
6250	2	6	0.5	No	6.11	———	2.02	5.1
3125	2	6	0.5	Yes	7.69	1.93	1.39	4.78
6250	2	6	1	Yes	8.58	4.25	1.53	4.77
3125	2	6	1	Yes	8.10	2.39	1.87	6.36

Figure 17 illustrates the dependence of the braking distance, the braking force in the first stage, and the time delay of activation of the second stage of braking.
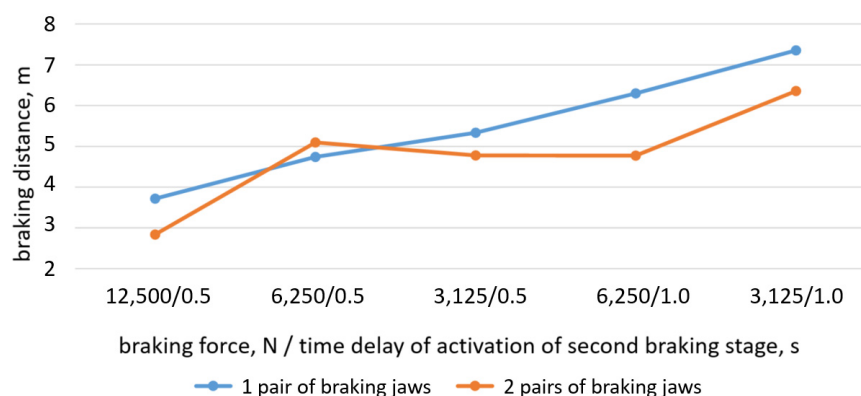

Figure 17. Diagram of the braking distance as a function of braking force and activation time delay (Reprinted from Ref. [32]).

Figure 18 illustrates the dependence of the maximum deceleration, the braking force in the first stage, and the time delay of activation of the second stage of braking.

The concept of the algorithm is an attempt to increase the safety of users of mine suspended transport. It is aimed at minimizing the dynamic overloads affecting people in the transport set. The action of these overloads may result in uncontrollable changes in the miner's body's posture and movement within the cabin, which could cause injury.

Based on the numerical simulations, it can be assumed that, for the studied suspended monorail system, setting the delay time in the range of 0.3–0.5 s and the deceleration threshold at the level of 4 ms^{-2} will enable the proper braking process during an emergency stop. Emergency braking in different conditions, such as braking on a horizontal and inclined (30°) routes, may result in introducing additional parameters into the algorithm, e.g., information about the current position of the drivetrain (articulation from the vertical position).
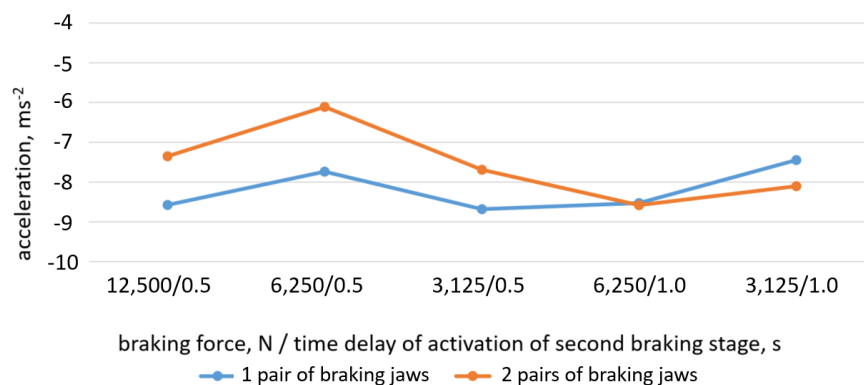
Figure 18. Diagram of the maximum deceleration as a function of braking force and activation time delay (Reprinted from Ref. [32]).

4.3. Making the Suspensions of the Operator's and Passenger's Cabins More Flexible

Another aspect that has a large impact on the comfort and safety of the crew transported by suspended monorails are vibrations in the operator's cabins and passengers' cabins while traveling. Passage through rail connections, imperfections in the route installation, as well as movement of the route during operation are the sources of vibrations. Rollers of suspended monorail, made of steel and moving on a steel rail, contribute significantly in generating the vibrations. Even slight irregularities (e.g., rail joints) or dirt on the rail can be a source of vibrations that are transferred to the machine and operator. The level of vibrations is important when taking into account time of exposure to vibration (train travel time), as well as the aspect of increasing the permissible speed (change of frequency and amplitude of vibrations). As part of the research work of the KOMAG Institute, a new type of yielding suspension of the passenger cabin and use of the inserts damping the vibrations in the operator's cabin were developed together with the monorail manufacturer. In addition, different types of elastic inserts made of different materials of different stiffness were tested. On this basis, the most suitable material that best reduced the transmission of vibrations from the chassis to the monorail operator available on the market was selected [33,34]. In order to analyse the effectiveness of such a solution, numerical simulations were carried out consisting in the passage of a suspended monorail set through a horizontal section of the route. During the simulation, the train set accelerated from 0 s to 0.2 s to the speed of $3.5 \, \text{ms}^{-1}$. Then, the set moved at a constant speed. While simulating, accelerations acting in cabins in three directions in accordance with the Cartesian coordinate system (X axis perpendicular to the direction of travel of the cable car, axis Y—consistent with the direction of travel of the cable car, axis Z—vertical axis) were recorded. A comparison of accelerations acting in the passenger cabin in the case of a monorail travel with not cushioned cab suspension (variant 1) and yielding suspension (variant 2) is shown in Figures 19–21.
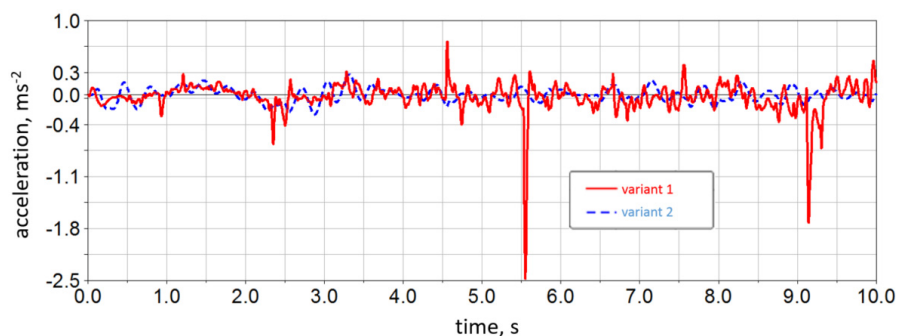

Figure 19. Passenger's cabin acceleration (X-axis) vs. time (Reprinted from Ref. [7]).
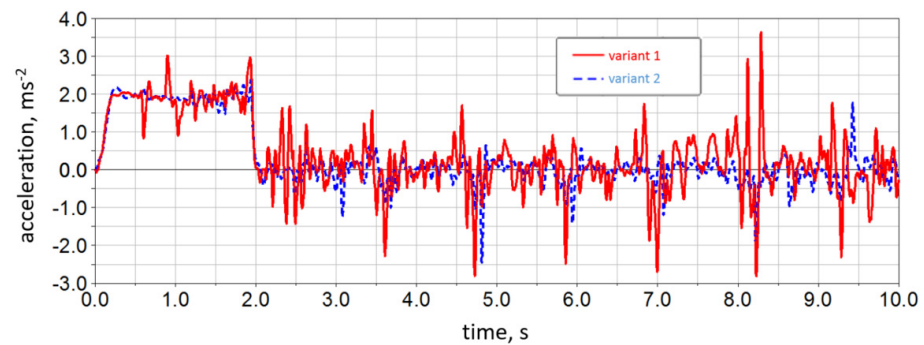
Figure 20. Passenger's cabin acceleration (Y-axis) vs. time (Reprinted from Ref. [7]).
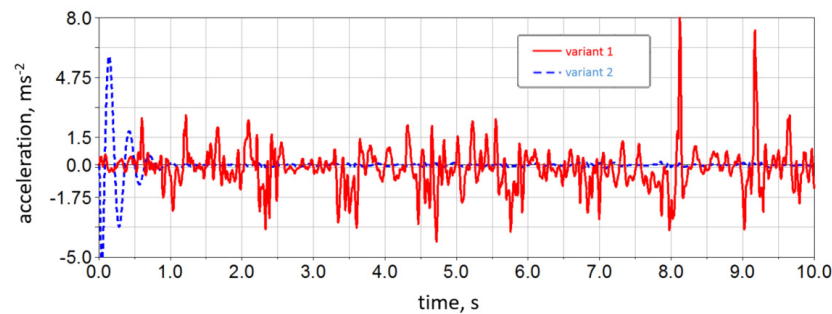

Figure 21. Passenger's cabin acceleration (Z-axis) vs. time (Reprinted from Ref. [7]).

Root mean square (RMS) accelerations of the operator's cabin and the passenger cabin in three directions (X-axis, Y-axis, Z-axis) is another result of the simulations. The RMS values are presented for the simulation of entire passage and for the passage of the monorail at a constant speed, excluding the acceleration phase (2 s–10 s). These results are presented in Table 13.

Table 13. Root mean square (RMS) accelerations in relation to the cabins (Reprinted from Ref. [7]).

	RMS of the X-axis, m·s^{-2}	RMS of the Y-axis, m·s^{-2}	RMS of the Z-axis, m·s^{-2}
	Operator's cabin		
variant 1—full	0.26	1.50	2.00
variant 1—2 s–10 s	0.17	1.41	2.18
variant 2—full	0.27	1.11	0.86
variant 2—2 s–10 s	0.18	0.82	0.89
	Passengers' cabin		
variant 1–full	0.21	1.03	1.13
variant 1—2 s–10 s	0.23	0.68	1.21
variant 2—full	0.09	0.88	0.69
variant 2—2 s–10 s	0.09	0.35	0.06

Then, in accordance with the provisions of the standard (PN-EN 14253+A1:2011), the daily exposure to vibration was calculated (A(8)). The calculations were performed on the assumption of an 8-h workday, during which the suspended monorail operator was exposed to cabin vibrations for 4 h, while passenger exposure time was supposed to be 2 h, as shown in Table 14.

Table 14. Daily exposure to vibrations on the operator and passenger of the suspended monorail (Reprinted from Ref. [7]).

	Ax(8), m·s^{-2}	Ay(8), m·s^{-2}	Az(8), m·s^{-2}	A(8), m·s^{-2}
Operator's cabin (exposure time 4 h)				
variant 1—full	0.25	1.49	1.42	1.49
variant 1—2–10 s	0.17	1.39	1.54	1.54
variant 2—full	0.26	1.09	0.6	1.09
variant 2–2–10 s	0.18	0.8	0.64	0.8
Passenger cabin (exposure time 2 h)				
variant 1—full	0.14	0.72	0.56	0.72
variant 1—2–10 s	0.16	0.48	0.6	0.6
variant 2—full	0.06	0.62	0.34	0.62
variant 2—2–10 s	0.06	0.24	0.03	0.24

Based on an analysis of the results, it can be stated that the solutions introduced to increase the flexibility of the suspension of the operator's cabin and the passenger cabin have a positive impact on the intensity of vibrations felt by the crew. This means that the vibrations are reduced, increasing the safety and comfort of suspended monorail users in underground mines.

4.4. Ergonomic Analyses of New Design Solutions for Passenger Cabins

As part of the development of the suspended monorail system, more and more attention is paid to the comfort and ergonomics of travel in these means of transport [35]. At the stage of developing a new design of the passenger transport cabin, ergonomic analyses of the selected designs of these cabins were carried out. As a result of the analyses, the static discomfort coefficient was determined for different sections of the spine. Figure 22 shows two designs of the passenger transport cabin.
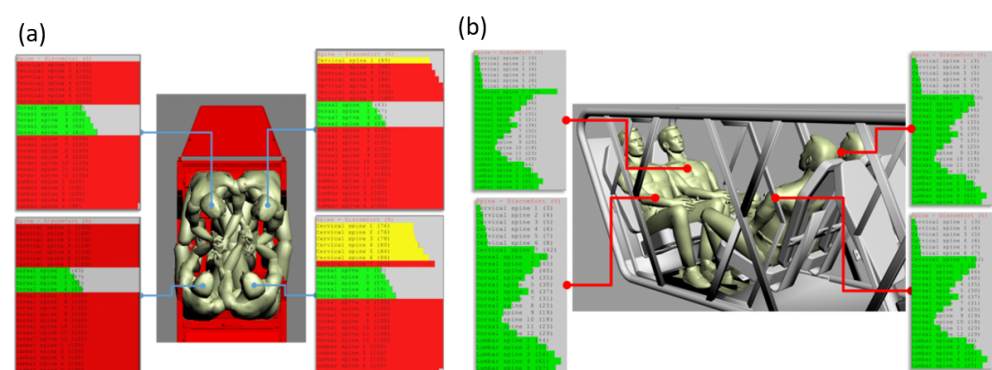
Figure 22. Values of the static discomfort coefficient for various sections of the spine; (**a**) previous version of the cabin; (**b**) the new version of the cabin [25].

As a result of the introduced design changes, the same number of people traveling in the passenger cabin has much more comfortable conditions and less strain on the spine.

4.5. Introduction of Seat Belts to the Operator Cabin

To improve the safety of the operator in the cabin in a dangerous situation, such as emergency braking or collision of the transport unit with a stationary obstacle, numerical simulations were carried out using the ATB model of anthropometric features. To conduct this part of numerical analysis the Patran (pre- and post-processor) and Dytran (explicit solver) software were used.

In the next stages of the work, it was suggested to equip the operator's cabin with seat belts. For this purpose, a comparative simulation was carried out along with the determination of the HIC (Head Injury Criterion) coefficient when the cabin hit an obstacle at the speed of 5 ms^{-1}, when the operator has a seat belt and without one. The visualization of the simulation results is shown in Figure 23.
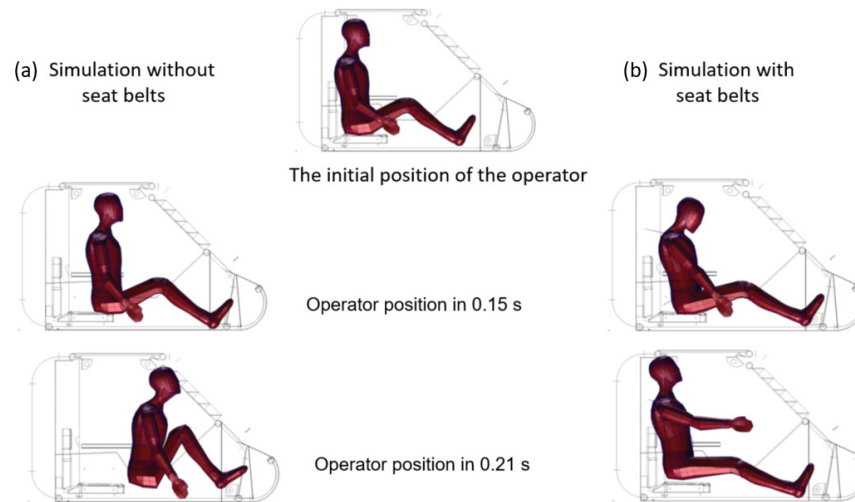

Figure 23. Position of the Hybrid III dummy when the cabin hits an obstacle at the speed of 5 ms^{-1}: (**a**) simulation without seat belts, (**b**) simulation with seat belts (Reprinted from Ref. [30]).

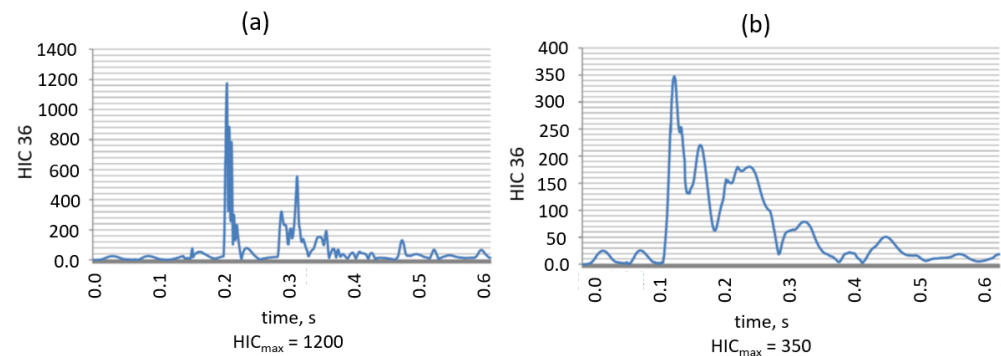A graph of HIC value determined in both versions of the simulation is presented in Figure 24.

Figure 24. Simulation results (HIC parameter) with speed of 5 ms^{-1}; (**a**) without seat belts; (**b**) with seat belts (Reprinted from Ref. [30]).

The operator's cabin should have additional passive safety features, such as seat belts or headrests, according to simulations conducted using the virtual Hybird III dummy and results analysis. In an emergency, these components will shield the operator from severe or even fatal injuries. Suggested additional equipment in the operator's cabin significantly decreases the HIC value, which should be considered to be minimizing the possibility of severe head injuries.

5. Conclusions

The numerical simulations results, as well as stand tests and in-situ tests, indicate the possibility of increasing the speed while transporting people in a safe way. Increasing the travel speed to 3 ms^{-1} is possible after prior verification of the design and straightness of the selected sections of the route on which the transport is planned. On the other hand, a further increase in travel speed, i.e., to 5 ms^{-1} and more, will require a quantitative assessment of

the quality of the route installation (e.g., ensuring straightness, protection against lateral swinging, small angular differences between adjacent rails), both before acceptance of a given section to operation and cyclically during its operation. Due to the high length of the routes in the underground mines and the need to make an assessment within an acceptable time, this will require the development of a special device (an inspection unit) moving on rails.

In special cases, where additional stabilization of the route will be required, while maintaining its yielding, the elastic and damping systems should be introduced to the stabilizing lashings. These systems, in the case of emergency braking of the transport unit, minimize the negative impact, i.e., they protect the joints, suspensions, and, ultimately, the roadway support frame against dynamic overload. The need to modify the braking systems of the suspended monorail drivetrain is another aspect that should be taken into account. Due to the fact that the kinetic energy of a moving object increases with the square of the increase in speed, these systems should be modified so that the temperature of 150 °C on the surface of the braking system actuators is not exceeded. This can be achieved by increasing the friction surface of the brake shoes, introducing active cooling of the brake shoes, and by enclosing the friction surfaces in the enclosure with an additional oil bath.

It should be emphasized that an increase in the speed of suspended monorails will take place in the selected areas of underground workings, characterized by a slight longitudinal inclination and no bends or junctions. Constraints regarding the inclination of the working are associated with the existing restrictions on pollutant emissions and the generation of additional heat as a factor causing an increase in temperature in the working environment, which discourages mines from using high-capacity and high-power drivetrains.

Institutional Review Board Statement: Not applicable.

Informed Consent Statement: Not applicable.

Data Availability Statement: Not applicable.

Conflicts of Interest: The authors declare no conflict of interest.

References

1. Pieczora, E.; Tokarczyk, J. Development of mine underground transportation with use of suspended monorails. *Min.-Inform. Autom. Electr. Eng.* **2017**, *4*, 96–117. [CrossRef]
2. Lutyński, A. KOMAG activities in the domestic and international research areas. *Min. Mach.* **2021**, *4*, 47–60. [CrossRef]
3. Becker, F.; Zell, M. The state of the art in positively guided rail transport systems for underground mining. *Min. Rep.* **2014**, *105*, 34–46. [CrossRef]
4. Jagoda, J.; Hetmańczyk, M.; Stankiewicz, K. Dispersed, self-organizing sensory networks supporting the technological processes. *Min. Mach.* **2021**, *2*, 13–23. [CrossRef]
5. Stankiewicz, K. Mechatronic systems developed at the KOMAG. *Min. Mach.* **2020**, *2*, 58–68. [CrossRef]
6. Song, Z.A.; Jiang, F. Hydraulic system elaboration and simulation for single-drive light-load monorail locomotive in fully mechanized coal mining applications. *IOP Conf. Ser. Mater. Sci. Eng.* **2019**, *474*, 012006. [CrossRef]
7. Szewerda, K.; Tokarczyk, J.; Bożek, P.; Michalak, D.; Drwięga, A. Vibrations diagnostics and analysis in operator's and passenger cabins of a suspended monorail. *Acta Montan. Slovaca* **2020**, *2*, 150–158. [CrossRef]
8. Regulation of the Minister of Energy "on Detailed Requirements for Conducting Underground Mining Plant Operations", November 23, 2016 (Journal of Laws of 2017, Item 1118) (Rozporządzenie Ministra Energii z Dnia 23 Listopada 2016 r. w Sprawie Szczegółowych Wymagań Dotyczących Prowadzenia Ruchu Podziemnych Zakładów Górniczych (Dz. U. z 2017 r. poz. 1118)). Available online: https://isap.sejm.gov.pl/isap.nsf/DocDetails.xsp?id=WDU20170001118 (accessed on 3 April 2023).
9. Danelson, K.A.; Golman, A.; Kemper, A.; Gayzik, F. Finite element comparison of human and Hybrid III responses in a frontal impact. *Accid. Anal. Prev.* **2015**, *85*, 125–156. [CrossRef]

10. Lai, X.; Wang, Y.; Zhou, Q.; Lin, Z.; Culiere, P. Development of a finite element pam-crash model of hybrid III anthropomorphic test device with high fidelity. In Proceedings of the International Technical Conference on the Enhanced Safety of Vehicles (ESV), Washington, DC, USA, 13–16 June 2011; p. 11-0031.

11. Tokarczyk, J. Method for identification of results of dynamic overloads in assessment of safety use of the mine auxiliary transportation system. *Arch. Min. Sci.* **2016**, *61*, 765–777. [CrossRef]

12. Tokarczyk, J. Method for virtual prototyping of cabins of mining machines operators. *Arch. Min. Sci.* **2015**, *60*, 329–340. [CrossRef]

13. Żuchowski, A. Analysis of the influence of the impact speed on the risk of injury of the driver and front passenger of a passenger car. *Eksploat. Niezawodn.—Maint. Reliab.* **2016**, *18*, 436–444. [CrossRef]

14. Wicher, J.; Więckowski, D. Influence of vibrations of the child seat on the comfort of child's ride in a car. *Eksploat. Niezawodn.— Maint. Reliab.* **2010**, *4*, 102–110.

15. Kowalski, P.; Zając, J. Research on simultaneous impact of hand-arm and whole-body vibration. *Int. J. Occup. Saf. Ergon.* **2012**, *18*, 59–66. [CrossRef]

16. Kowalski, P.; Zając, J. Influence of vertical and horizontal whole body vibration on some psychomotor and cognitive functions of employees age 50+ (pilot study). *J. Vibroeng.* **2017**, *19*, 2174–2179. [CrossRef]

17. Kiełbasa, P.; Dróżdż, T.; Wojtas, D. Analiza drgań ogólnych i miejscowych na stanowisku pracy operatora specjalistycznej maszyny drogowej. *Autobusy* **2019**, *1–2*, 281–286. [CrossRef]

18. Bovenzi, M. Health effects of mechanical vibration. *G. Ital. Med. Lav. Ergon.* **2005**, *27*, 58–64. [PubMed]

19. Krajnak, K. Health effects associated with occupational exposure to hand-arm or whole body vibration. *J. Toxicol. Environ. Health* **2018**, *21 Pt B*, 320–334. [CrossRef]

20. Basri, B.; Griffin, M.J. Predicting discomfort from whole-body vertical vibration when sitting with an inclined backrest. *Appl. Ergon.* **2013**, *44*, 423–434. [CrossRef]

21. Horyl, P.; Šňupárek, R.; Maršálek, P.; Poruba, Z.; Pacześniowski, K. Parametric Studies of Total Load-Bearing Capacity of Steel Arch Supports. *Acta Montan. Slovaca* **2019**, *24*, 213–222.

22. Pytlik, A.; Rotkegel, M.; Szot, Ł. Badanie wpływu prędkości kolejek podwieszonych na siły w wybranych elementach trasy. *Przegląd Górniczy* **2016**, *11*, 30–37.

23. Pytlik, A. Tests of steel arch and rock bolt support resistance to static and dynamic loading induced by suspended monorail transportation. *Stud. Geotech. Mech.* **2019**, *41*, 81–92. [CrossRef]

24. Tokarczyk, J.; Rotkegel, M.; Pytlik, A.; Niedworok, A. Research on the impact of forces and acceleration during the riding and braking of a suspended monorail. *Arch. Min. Sci.* **2020**, *65*, 399–414. [CrossRef]

25. INESI European Project: Increase Efficiency and Safety Improvement in Underground Mining Transportation Routes. RFCS, 2017–2020, Contract No. 754169. Available online: https://komag.eu/aktualnosci/2396-realizacja-projektu-europejskiego-inesi (accessed on 23 April 2023).

26. Szewerda, K.; Tokarczyk, J.; Pytlik, A. Suspended monorail emergency braking trolley computational model verification based on bench tests. In Proceedings of the Mining of Sustainable Development, Gliwice, Poland, 28 November 2018; Volume 261. [CrossRef]

27. Pytlik, A.; Tokarczyk, J.; Frąc, W.; Michalak, D. Explosive atmosphere ignition source identification during mining plant suspended monorail braking unit operation. *Acta Montan. Slovaca* **2021**, *26*, 338–351. [CrossRef]

28. Herbuś, K.; Szewerda, K.; Świder, J. Virtual prototyping of the suspended monorail in the aspect of increasing the permissible travel speed in hard coal mines. *Eksploat. Niezawodn.—Maint. Reliab.* **2020**, *22*, 610–619. [CrossRef]

29. Szewerda, K.; Tokarczyk, J.; Wieczorek, A. Impact of Increased Travel Speed of a Transportation Set on the Dynamic Parameters of a Mine Suspended Monorail. *Energies* **2021**, *14*, 1528. [CrossRef]

30. Szewerda, K.; Tokarczyk, J.; Świder, J.; Grodzicka, A. Impact of suspension and route stabilization on dynamic parameters of self-driven mine suspended monorails. *Eksploat. Niezawodn.—Maint. Reliab.* **2022**, *24*, 617–628. [CrossRef]

31. Załącznik nr 2 do Rozporządzenia Rady Ministrów z dnia 30 kwietnia 2004 r. w sprawie dopuszczania wyrobów do stosowania w zakładach górniczych. *Dz. Ustaw* **2004**, *99*, 6870–6930.

32. Świder, J.; Szewerda, K.; Herbuś, K.; Jura, J. Testing the Impact of Braking Algorithm Parameters on Acceleration and Braking Distance for a Suspended Monorail with regard to Acceptable Travel Speed in Hard Coal Mines. *Energies* **2021**, *14*, 7275. [CrossRef]

33. Szewerda, K. Supporting development of suspended underground monorails using virtual prototyping techniques. In Proceedings of the Innovative Mining Technologies (IMTech Scientific and Technical Conference), Szczyrk, Poland, 25–27 March 2019; Volume 545. [CrossRef]

34. Świdra, J. (Ed.) *Drgania Układów Zdyskretyzowanych z Symulacją Komputerową*; Monografia: 877; Wydawnictwo Politechniki Śląskiej: Gliwice, Poland, 2021; ISBN 978-83-7880-745-2.

35. Tokarczyk, J.; Michalak, D.; Rozmus, M.; Szewerda, K.; Żyrek, L.; Zeleznik, G. Ergonomics assessment criteria as a way to improve the quality and safety of people's transport in underground coal mines. In Proceedings of the AHFE Conference 2019, Washington, DC, USA, 24–28 July 2019; pp. 305–317.